10
Emerging Network Activity in Dissociated Cultures of Neocortex: Novel Electrophysiological Protocols and Mathematical Modeling

Michele Giugliano, Maura Arsiero, Pascal Darbon, Jürg Streit, and Hans-Rudolf Lüscher

Introduction

10.1 Outline

Since the early attempts at combining micro-fabricated transducers with in vitro neurobiological systems (Gross, 1979; Gross et al., 1985), cultures of neurons dissociated from the vertebrate nervous system have represented a convenient choice for several reasons (Stengler and McKenna, 1994). Neurons can be easily cultured over biocompatible substrates, grown in an incubator and maintained under healthy conditions for several weeks or more (Potter and DeMarse, 2001). This fulfills the requirements of the unconventional approach followed by MEA investigators: instead of invasively probing a single neuron by means of (e.g.) an intracellular glass-pipette electrode, let a population of neurons develop ex vivo and grow around multiple probes, for extended periods of time, under noninvasive conditions. On the other hand, the choice of cultured neurons is also related to the in vitro development of functional synaptic contacts (Nakanishi and Kukita, 1998) and to the emergence of spontaneous patterned electrical activity (Kamioka et al., 1996; Van den Pol et al., 1996). Thus, along a tradition of investigation that is common to physics (Amit, 1989), the possibility of accessing a reduced version of an active nervous system (Bulloch and Syed, 1992) constitutes a unique opportunity for the investigation of network electrophysiology. Indeed, such an approach makes it possible to dissect the interactions among individual neurons of a network and to look for collective mechanisms at the cellular and subcellular levels, through manipulation of the physicochemical conditions.

Under such perspectives, we review in this chapter electrophysiological data obtained from networks of neurons dissociated from the rat neocortex and cultured over arrays of substrate micro-electrodes (MEAs). In particular, we discuss a recent

This chapter is dedicated to the memory of the late Professor Massimo Grattarola, who pioneered the MEA technique in Italy.

experimental approach for the study of cortical network electrophysiology, and introduce a simple theory accounting for the emergence of the in vitro spontaneous collective activity. We conclude with some remarks on the perspectives of novel experimental protocols and mathematical modeling, as complementary tools to MEAs and traditional electrophysiological techniques.

10.1.1 Relevance of the Study of In Vitro Neocortical Networks

In the field of life sciences, we are assisting in an increase of interest for the function of biological networks of elements and for the complexity emerging from the interactions and combinations of such elements (e.g., the dynamics of motifs in neuronal/genetic/metabolic/biochemical networks) (Milo et al., 2002). The underlying inspirations of such a trend suggested interesting analogies with the physics of semiconductors and with the development of modern digital electronics (Grattarola and Massobrio, 1998). In fact, the design of semiconductor electronics proceeded first from very simple devices interconnected in complex manners (i.e., transistors and Boolean logic-gate networks), then evolved into a relatively simple interfacing of highly sophisticated units (e.g., cluster computing, parallel architectures, etc.).

In the case of the design of biological systems, evolution followed an opposite path. It started from the simple combination of complex (bio)molecular compounds (e.g., the assembly of a lipidic bilayer) and went on, assembling the nervous system of mammals, which functionally appears as a highly intricate map of networks, each composed of complex (sub)cellular elements. However, the most recent phylogenic outcome of evolution, the neocortex, might reveal simpler principles (Douglas and Martin, 1990), irrespective of its anatomical complexity and heterogeneity. In addition, the very same basic electrophysiological processes might be carried out by each small region of the neocortex, by a kind of general-purpose canonical micro-circuitry. Actually, although there are several differences from layer to layer, with regard to projections, cell density, morphology, and size, a stereotypical organization seems indeed to dominate. For instance, Douglas and Martin (1990) focused their proposal on a canonical building block, underlining and emphasizing the tremendous recurrent excitation, estimated as 90% of the total afferent excitation.

In such a context, and under the perspective of ultimately understanding how the synaptic organization of the neocortex produces the complexity of cortical functions, the convergence of a mathematical theory and experimental results is imperative. Such an approach might be also devised to determine how many of the details underlying single channels, dendrites, neurons, and synapses, play a role at higher levels, and whether these details must be fully retained or largely simplified, at the level of large-scale cortical processing description.

One possibility to challenge existing theories and to develop new ones, is represented by the study of in vitro preparations as reduced and highly simplified neurobiological systems, with regard to the network-level electrical activity.

Nevertheless, in vitro networks are generally not considered to retain enough details and features of the in vivo cortical physiology (Steriade, 2001). This is certainly true with regard to differences in neuronal morphology, firing patterns, and resting properties, as well as in functional aspects and oscillatory organized activities. In the case of cultured networks of dissociated cells, the bidimensional arrangement of random synaptic contacts might be a reason for further skepticism.

However, keeping in mind such limitations and avoiding the tempting attitude of incriminating isolated neuronal properties, channels, and molecules as responsible for complex physiological or behavioral processes, in vitro preparations might still be invaluable research tools. Although cellular diversity and differentiation are retained in cultures (Huettner and Baughman, 1986), it is very unlikely that the precise "signature" of any canonical micro-circuitry is reproduced, as neuronal connections randomly re-organize. However, strong excitatory recurrent coupling characterize in vitro cultures (Nakanishi et al., 1999), and forms of collective electrical activities arise spontaneously, sustained by recurrent synaptic connections (Maeda et al., 1995). These constitute intermediate steps of investigation, crucial to the understanding of in vivo cortical phenomena. Therefore, the inaccuracy of in vitro networks in re-creating faithful replicas of in vivo functions may not represent an obstacle and, on the contrary, it is an ideal framework to develop novel electrophysiological protocols and test theoretical interpretative frameworks.

In such a context, the MEA technique, by increasing the spatial resolution and making it possible to chronically and noninvasively track collective network activity over time, is playing an instrumental role. Referring again to the analogy with digital electronics, the availability of MEAs is providing the conditions for accessing the simultaneous electrical activity of several components, interconnected in a functional circuit. We believe that a step in the direction of understanding the general principles underlying the design of "digital computers" (the design of a neocortex) may come from the understanding of how a subset of "transistors" and "diodes" (neurons and synapses) performs concerted and not isolated functions.

10.2 MEA Experiments

10.2.1 Culture Technique, MEA Recordings, and Single-Neuron Patch-Clamp

According to standard methods, cortical neurons can be enzymatically dissociated from the cortices of early postnatal rats, by exposing brain tissue slices to a trypsin solution. After such a treatment, cells completely lose neurites and synaptic connections and are plated on a MEA surface (Tscherter et al., 2001), previously coated with substances promoting cell adhesion (Stengler and McKenna, 1994). After just a few hours from plating, neurons start to elongate new neurites, establish synaptic contacts, and, after a few weeks in culture, reach a mature stage (Kamioka et al., 1996), and self-organize into a densely interconnected cellular monolayer. Axonal and dendritic branches at this stage extend over 1 mm, resulting in a large

number of functional synapses with neighboring cells (Marom and Shahaf, 2002; Nakanishi and Kukita, 1998).

As already mentioned, by culturing dissociated neurons over MEAs, neuronal somata as well as axons are allowed to develop close to the individual substrate micro-electrodes. Such proximity makes it possible to extracellularly detect spontaneous spiking activity from one or more neighboring cells (Streit et al., 2001; Bove et al., 1998; Grattarola and Martinoia, 1993). As this kind of signal transduction procedure is noninvasive, electrical activity of in vitro networks can be characterized as it progresses, evolves, and organizes, during long-term culture, while preserving sterile and physiological conditions.

The MEAs employed in our experiments contained 68 platinum planar electrodes, spaced 200 μm and laid out in the form of a rectangle. During each recording session, channels showing neuronal activity were selected and recordings were digitized to be stored on a hard disk, while monitoring multi-channel amplified raw voltage traces with a custom oscilloscope software. The detection of extracellularly recorded action potentials (i.e., fast voltage transients) and further analysis were performed offline as previously described (Giugliano et al., 2004; Tscherter et al., 2001; Streit et al., 2001). In a series of experiments, a patch-clamp technique was employed in the whole-cell configuration (Hamill et al., 1981). The aim of these experiments was to access the intracellular membrane voltage at the soma of cultured neurons, and to characterize single-cell responses to current injection. Therefore, network activity had to be suppressed by a cocktail of blockers of synaptic transmission. This consisted of D-2-amino-5-phosphonovalerate (D-APV) and 6-cyano-7-nitroquinoxaline-2,3-dione (CNQX), which are competitive antagonists of the NMDA and non-NMDA glutamatergic receptors, respectively. Once these substances were bath-applied, incoming synaptic activity and spontaneous spiking were completely suppressed (see next sections and Figure 10.1). Such a pharmacological manipulation makes it possible to study electrical properties of individual neurons, under isolated conditions, as neurons receive no inputs from the surrounding network, other than what is artificially injected through the patch-pipette by the experimenter.

10.2.2 Development of In Vitro Electrical Activity

Before about seven days in vitro (DIV), most neurites do not reach neighboring neurons (Nakanishi et al., 2001) and the distributed electrical activity consists in the emission of rare action potentials, as detected by individual MEA electrodes (Kamioka et al., 1996). No spatial propagation of signals is observed at this stage and no correlation characterizes neuronal activity at spatially distinct locations. Such spontaneous activity is completely abolished by tetrodotoxin (TTX), a blocker of intrinsic neuronal spiking mechanisms, or by selective antagonists of glutamatergic synaptic receptors or by activation of GABAergic receptors (Kamioka et al., 1996). This evidence suggests that at this stage, the network can be regarded as an arrangement of uncoupled neurons, whose membrane voltage rarely fluctuates, reaching an excitability threshold as a result of spontaneous synaptic receptor activation.

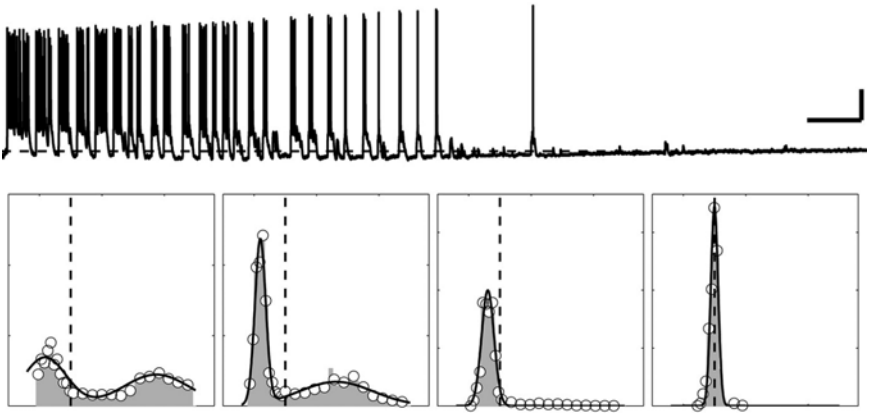

FIGURE 10.1. Synaptic bases of network-driven population bursts. A cocktail of pharmacological blockers of fast excitatory synaptic transmission was bath-applied while recording intracellularly the membrane voltage of a neuron participating to population bursting (upper trace, over 80 sec). As time passes and the number of blocked synaptic receptors increases to saturation, the coupling between neurons of the network becomes weak and finally breaks, as no PB occurs anymore. As the network synaptic drive decreases, a hyperpolarizing contribution fades out, releasing resting membrane voltage to slightly more depolarized values (dashed line). Finally, the cumulative inactivation (see Figure 10.8) of spike-emission processes recovers, and the over-shoot amplitude of individual action potentials increases as the fraction of inactive sodium channels decreases. Under these conditions, the subthreshold voltage amplitude histogram was computed every 20 sec (lower panels: bars and circles): at the beginning the distribution is well fitted (thick lines) by a double Gauss-function and later by a single Gauss-function, while its mean slightly shifts to more depolarized values (calibration: 5 sec/ 20 mV for the upper trace, 9 mV/0.05 mV^{-1} for the two lower-left panels and 9 mV/0.12 mV^{-1} for the others).

Spontaneous presynaptic leakage of neurotransmitter molecules or glutamate spill-over from neighboring synapses can explain such an activity phase (Maeda et al., 1995). Such random uncorrelated firing evolves, at a later stage, into a more organized firing pattern, consisting of isolated spikes and quite regular sequences of bursts of action potentials. These bursts, referred to as population bursts (PBs), occur almost simultaneously across all the MEA micro-electrodes and are not characterized by reproducible spatial trajectories, while propagating across the network (Maeda et al., 1995). This phase characterizes cultured networks around 5 to 16 DIV and it is associated with structural changes, represented by an increase in neurite elongation and by the formation of functional synapses (Nakanishi et al., 2001; Nakanishi and Kukita, 1998). Individual neurons emit rare and irregular spikes or bursts of action potential, superimposed on spontaneous voltage fluctuations around a resting potential of about −60 mV (Nakanishi and Kukita, 1998), similarly to what is observed in adult neocortex (Sanchez-Vives and McCormick, 2000). As time in cultures further advances, the propagation velocity of PBs across the network increases, indicating the formation of an increasing number of reliable synaptic connections. After about 30 DIV, the network reaches a stable condition

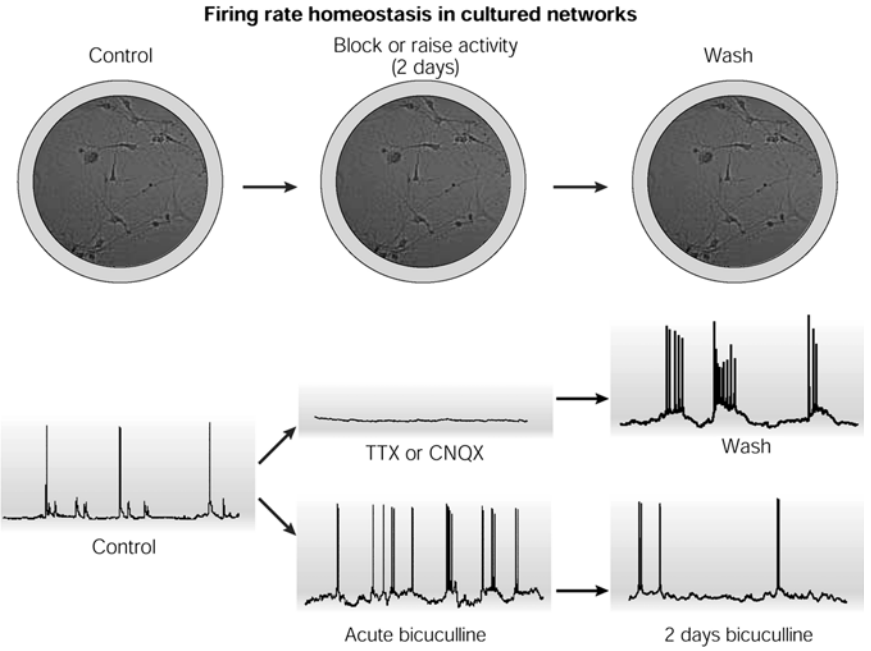

FIGURE 10.2. In vitro chronic pharmacological manipulation of synaptic transmission in cultured networks of neocortical neurons induces rebound phenomena as soon as control conditions are restored. Homeostatic mechanisms of the population firing rate therefore coexist with heterosynaptic plasticities and participate in adjusting cellular and synaptic properties, to compensate for changes in synaptic drive. As a consequence, single-neuron properties as well as synaptic efficacies are dynamically regulated over time scales ranging from hundreds of milliseconds to minutes and hours, in activity-dependent manners. (Reproduced with permission from *Nature Reviews Neuroscience*; © 2004 Macmillan Magazines Ltd.)

of maturation, exhibiting a richer and more elaborate temporal pattern of irregular, synchronized population bursts (Marom and Shahaf, 2002; Kamioka et al., 1996; Maeda et al., 1995). Maturation of the network is also associated with a transient decline in the number of synapses, which is markedly related to activity-dependent processes (Van Huizen et al., 1987) as well as homeostatic plasticity (Turrigiano and Nelson, 2004; see Figure 10.2).

10.2.3 Population Bursting Is Driven by Network Interactions

The available electrophysiological and pharmacological data convincingly suggest that the spontaneous electrical activity described above emerges as a collective phenomenon, and is sustained by synaptic connectivity (see Figure 10.3). No intrinsic neuronal pacemaker mechanisms have been reported so far, either to account for the random spatial features of the origin and propagation of population bursts (Maeda et al., 1995), or to explain correlations between collective activity and

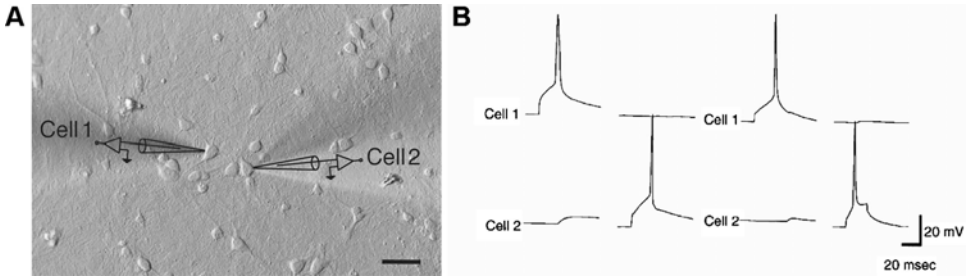

FIGURE 10.3. Cultured neurons, dissociated from neocortex, establish extensive functional chemical synapses, a few weeks after plating. These connections have been studied with simultaneous pair recordings by Nakanishi and collaborators (A) (calibration: 50 μm). Although in vitro connectivity appears to be higher than in intact cortex, emission of a spike by a presynaptic (excitatory) neuron usually evokes (B) weak subthreshold responses in postsynaptic cells, for unidirectional (left) as well as bidirectional coupling (right). (Modified and reproduced with permission, © 1998–1999 Elsevier Ltd.)

plastic changes in synaptic efficacy induced by repetitive electrical stimulation (Jimbo et al., 1999; Maeda et al., 1998). During the mature stage of these cultures, synaptic connectivity of a generic neuron has been estimated to be generally monosynaptic, with propagation delays of a few milliseconds, irrespective of the spatial distance between cells, and to involve 10 to 30% of other neurons (Nakanishi and Kukita, 1998).

Together with the large number of anatomical synaptic contacts (Marom and Shahaf, 2002), and the strong correlation between activity and degree of development of neurite outgrowth (Nakanishi et al., 2001; Kamioka et al., 1996; Muramoto et al., 1993), these considerations support a network architecture able to sustain a reverberating spiking activity through recurrent excitatory connections. Consistent with the in vitro connectivity pattern, relatively restricted to spatially neighboring sites, a mature cultured network could be therefore thought of as a homogeneous chain of synaptically connected subpopulations (Giugliano et al., 2004). Each population would then have some probability to initiate a PB, spreading to the entire culture by means of sparse excitatory connectivity. Physical network sectioning experiments of Maeda et al., (1995), and of Nakanishi and Kukita (1998) are consistent with such an interpretation and with the hypothesis that synchronized bursting is mediated by chemical synapses rather than by way of gap junctions and/or diffusible factors.

10.3 From Single-Neuron Properties to Network Activity

As the electrical activity described in the previous section is an emerging population phenomenon, it is relevant to investigate the quantitative conditions for its occurrence. It is also of particular interest for network neurosciences to characterize the cellular-level features of neurons and synapses, which play a major role

at the network level. In fact, it is likely that an effective description of neuronal integration and excitability at the cellular level will provide several benefits for the prediction of the population-level activity, in analogy to the outstanding contributions of the phenomenological (macroscopic) description of the ionic (microscopic) mechanisms proposed by Hodgkin and Huxley (1952) for the generation of an action potential. In particular, the characterization of single-neuron (input–output) response properties, carried out under the appropriate conditions, has been suggested as a fundamental step to predict and quantitatively interpret how a population of neurons interacts. Such a view is strongly supported by several theoretical studies (Salinas, 2003; Mattia and Del Giudice, 2002; Brunel, 2000), where single-neuron response properties have been exploited to derive predictions about collective phenomena, such as the global spontaneous irregular activity (Amit and Brunel, 1997), the emergence of fast network-driven oscillations (Brunel and Wang, 2003; Fuhrmann et al., 2002), and of selective delay-activity states (Wang, 2001; Amit and Brunel, 1997).

10.3.1 How Can We Re-Create a Realistic Input to an Isolated Neuron?

In vivo neocortical neurons continuously produce excitatory and inhibitory postsynaptic currents (EPSCs/IPSCs) (Destexhe and Paré, 1999). Such an intense activity arises from the high degree of connectivity of intracortical afferents, spontaneously active at very low firing rates, making postsynaptic membrane voltage fluctuate as in a random walk (Destexhe et al., 2003; Abeles, 1991; Gerstein and Mandelbrot, 1964). This phenomenon is known to strongly affect intrinsic biophysical properties of neurons, as compared to TTX-induced resting conditions, and to modulate their responsiveness to external inputs (Steriade, 2001; Gerstner, 2000; Destexhe and Paré, 1999). In such perspectives, traditional in vitro electrophysiological protocols, which consist in the evaluation of the transient spiking response to an injection of DC current steps (McCormick et al., 1985), are completely inappropriate to approach the single-neuron level (Holt et al., 1996).

Although it is apparent that the conditions in mature cultures are different from those of an intact cortex, these considerations still hold when considering emerging population activity. In particular, if we are to determine the effective single-neuron response properties, we must employ a protocol that replicates conditions experienced by the same neuron, when participating in the network activity. Thus, we immediately realize that nonstationarity characterizes the inputs to a neuron, during each PB (see Figure 10.1). The amplitude distribution of the subthreshold membrane voltage, recorded in current-clamp, indicates two alternating regimes: a resting condition, with low variance, and an active phase possibly related to a high-conductance state (Destexhe et al., 2003).

In the following, we consider only the active regime. In fact, invoking quasi-stationary conditions, we later recover the nonstationarity and ignore such a simplification (Giugliano et al., 2004). But how do we mimic all possible (stationary) inputs to the network? As described in the previous sections, the whole-cell

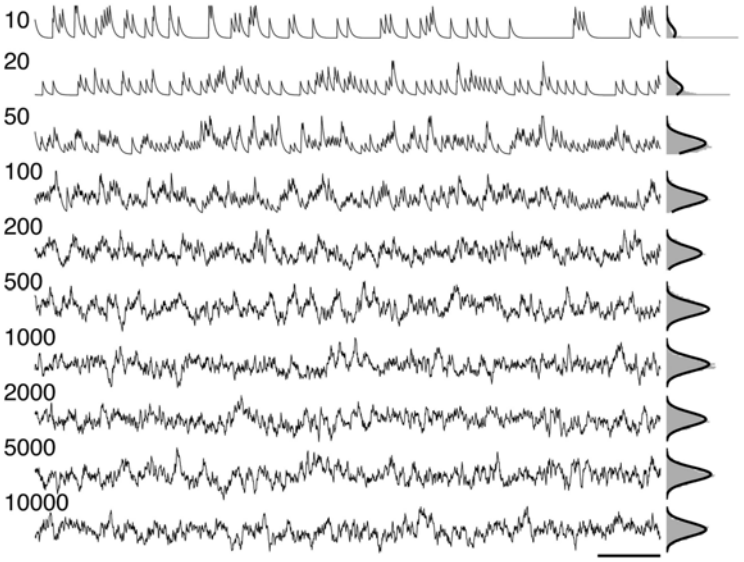

FIGURE 10.4. The overall synaptic input, resulting from stationary activation of a network of presynaptic neurons, can be described as a random walk in time and characterized by a Gauss-distributed stochastic process (i.e., by the central-limit theorem). The figure reports the computer-simulated time course of the total synaptic input to a generic neuron, quantified as conductance or current changes, from a presynaptic neuronal population of increasing size, through identical independent AMPAr-mediated synapses (i.e., 10–10,000, $\tau_I = 10$ msec). The distribution of amplitudes approaches a bell-shaped profile (panels on the right column) for as few as 100 synapses, each spontaneously active at a very low rate of 5 Hz (calibration: 100 msec).

patch-clamp technique can be exploited to inject a desired stimulus waveform into an isolated neuron and to measure the resulting input–output transformation. In the recent literature, there have been several attempts at re-creating in vitro a realistic network input (Silberberg et al., 2004; Chance et al., 2002; Fuhrmann et al., 2002; Protopapas and Bower, 2001; Destexhe and Paré, 2000; Poliakov et al., 1997; Mainen and Sejnowski, 1995). We followed Rauch et al. (2003), who proposed to computer-synthesize a Gauss-distributed noisy waveform and to inject it under current-clamp into the soma. Such nondeterministic stimuli are supposed to re-create realistic fluctuations for a cell embedded in a large cortical network (Figure 10.4; Destexhe et al., 2003).

10.3.2 The Extended Mean-Field Hypothesis

The theoretical framework, which inspires and motivates the approach of Rauch et al. (2003), is related to a powerful mathematical technique that makes it possible to predict the mean firing rate of a population of interacting neurons on the basis of the discharge response of a single cell to a realistic noisy input (Amit and Brunel,

1997). Further validating the hypotheses behind the use of noise injections, we note that there is a higher, and considerably less structured, degree of in vitro synaptic connections, compared to the in vivo cytoarchitecture. Moreover, because the impact of a single EPSC/IPSC on the in vitro postsynaptic membrane voltage is very weak in evoking suprathreshold responses (see Figure 10.3), the overall current experienced by a generic postsynaptic neuron can be indeed approximated by a diffusion stochastic process (see Figure 10.4 and Appendix; Fourcaud and Brunel, 2002; Destexhe and Paré, 2000).

Such considerations are linked to the hypothesis that individual neurons in a homogeneous active network cannot be distinguished in a statistical sense. In fact, because of the very large number of (random) synaptic connections and the presence of nonhomogeneities and noise sources, neurons roughly tend to instantaneously experience the same input current. Of course, each neuron will instantaneously receive a different realization of the same process, but its descriptors (i.e., current mean, variance, and correlation time length) are assumed to be the same. In other words, each neuron experiences the same mean field, extended to the regime of input fluctuations. Under such hypotheses, the characterization of the discharge properties of a single neuron becomes statistically representative of the others, as a whole.

10.3.3 The Noisy Current-Clamp Protocol

Because the nondeterministic stimuli described in the previous section account for different presynaptic network architectures and regimes, let's, for instance, indicate by $N_{e/i}$ the number of excitatory/inhibitory neurons, characterized by stationary mean activation rates $f_{e/i}$ and projecting to a generic neuron with probability $C_{e/i}$. Under the hypothesis that synaptic inputs are approximately independent, the distribution of the resulting postsynaptic somatic current amplitude becomes Gauss-distributed, by the central-limit theorem (see Figure 10.4), with steady-state mean m and variance s^2 given by the expressions reported below (Rauch et al., 2003):

$$\mathrm{m} = \mathrm{N_e C_e \langle I_e \rangle f_e \tau_e} - \mathrm{N_i C_i \langle I_i \rangle f_i \tau_i}$$

$$\mathrm{s^2} = \mathrm{N_e C_e \langle I_e^2 \rangle f_e \tau_e}/2 + \mathrm{N_i C_i \langle I_i^2 \rangle f_i \tau_i}/2$$

where $I_{e/i}$ and $\tau_{e/i}$ are the effective peak-amplitude and decay time constant at the soma, for individual excitatory and inhibitory postsynaptic currents, respectively, and the averaging operator $\langle\ \rangle$ is intended across the population of synapses. In this example, we can therefore inject a realization of a Gauss-distributed noisy current, characterized by (m,s^2), to recreate in an isolated neuron the input from such an afferent network.

In a more general case, in our experiments we aimed at an exploration of the plane (m,s^2), although some of the combinations might not be consistent with all possible network regimes. For any pair (m,s^2), an iterative expression was thus employed to synthesize a realization $I(t)$ of a current to be injected, under

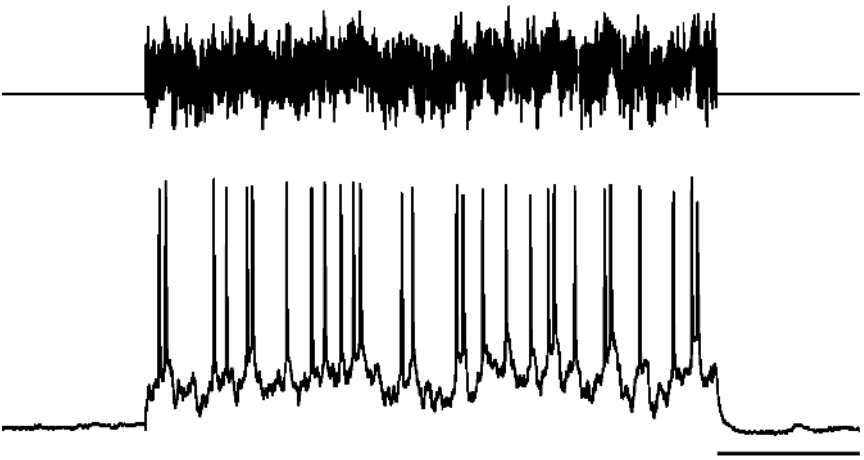

FIGURE 10.5. Electrical response evoked by a noisy stimulus current that mimics a realistic input drive of cortical networks. The response is determined by either mean current or random fluctuations. Each stimulus waveform was generated as an independent realization of the stochastic Ornstein–Uhlenbeck process, fully specified by the steady-state mean m, variance s^2, and autocorrelation time-length τ_I (calibration: 1 sec). (Modified and reproduced with permission, © 2004, The American Physiological Society.)

current-clamp, in the soma of patched neurons (see Figure 10.5):

$$\mathrm{I(t+dt) = I(t) + (m - I(t))\frac{dt}{\tau_I} + s\sqrt{\frac{2dt}{\tau_I}}\,\xi_t}, \tag{10.1}$$

where ξ_t is a unitary Gauss-distributed random variable (Press et al., 1992), updated at a rate of 5 kHz (i.e., $dt = 0.2$ msec). We fixed $\tau_e = \tau_I = \tau_I = 5$ msec, thereby focusing on AMPA- and $\mathrm{GABA_A}$-mediated synaptic currents (Destexhe et al., 1994). As a neuronal output, we chose to estimate the steady-state mean firing rate f as a function of m and s^2. Actually, $f(m, s^2)$ is the only relevant descriptor, under the assumption of the mean-field hypothesis, to predict the population firing rate (Amit and Brunel, 1997). Such a characterization allows us to predict, in a self-consistent way, how population activity occurs in a network of connected neurons, because the recurrent synaptic components can be described by recursively considering $m = m(f)$ and $s^2 = s^2(f)$ (Giugliano et al., 2004; Amit and Brunel, 1997).

10.4 Single Neurons Respond as Integrate-and-Fire Units

The results of single-neuron experiments have been summarized in Figures 10.6 and 10.7. As opposed to a DC stimulation, which elicits periodic and regular spike trains, noisy current injection produces neuronal membrane voltage that evolves

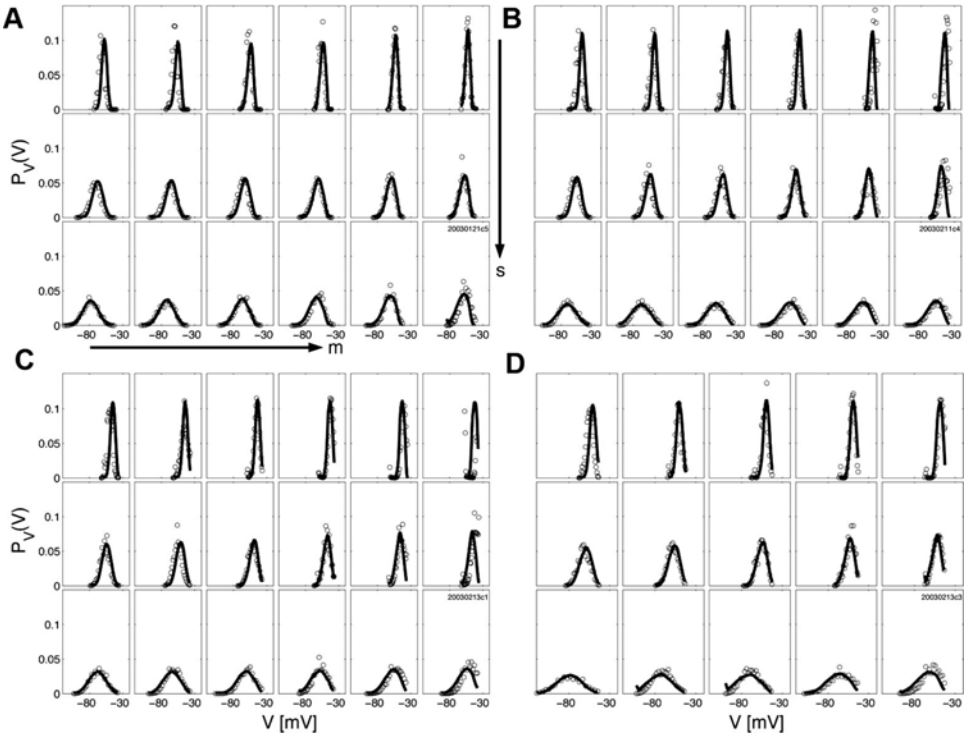

FIGURE 10.6. Steady-state amplitude distribution of subthreshold membrane voltage in single-cell noise injection experiments. The amplitude distribution of membrane voltage in single-cell noise injection experiments (open circles) is in good agreement with the mathematical model prediction (continuous thick line; see Appendix), although its parameters were tuned to match the mean firing rates only (see Figure 10.7 and compare to Figure 10.1). Panels A–D report the results from four different experiments, and in each subplot the voltage amplitude density distribution is plotted for increasing values of m, from left to right, and of s from top to bottom, within the same panel. (Reproduced with permission, © 2004, The American Physiological Society.)

in time as in a random walk, leading to an irregular spike emission (Figure 10.5). Its subthreshold amplitude distribution becomes bell-shaped, similar to what is observed in vivo (but see also Figure 10.1), with mean and standard deviation increasing with m and s^2 (see Figure 10.6). Cultured neurons also showed very similar response properties compared to neurons in acute slices (Rauch et al., 2003), when repetitively stimulated by the same noise realization. This was shown to yield a much higher precision in the timing of individual spikes in slices (Mainen and Sejnowski, 1995), proving that the somatic spike emission mechanism of cultured neurons is intrinsically reliable.

However, the most unexpected and interesting result is the following: as far as the steady-state spiking frequency f is concerned, cultured neocortical neurons

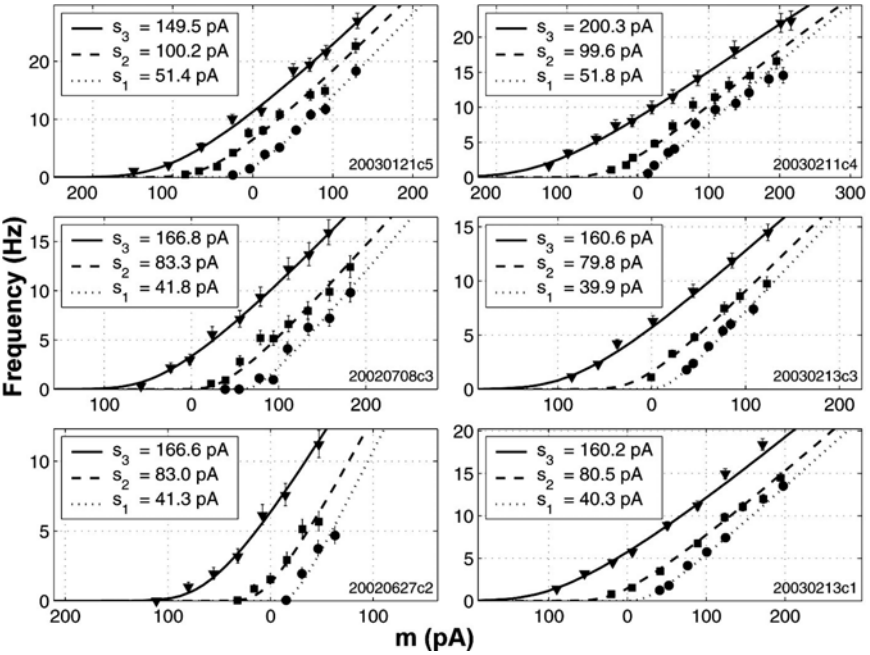

FIGURE 10.7. Results from six different single-cell noise injection experiments (see Figure 10.5). The current-to-discharge rate response of cortical neurons is captured with remarkable accuracy in the plane (m,s^2) by the simplified dynamics of a leaky integrate-and-fire model neuron. Experimental responses were evaluated at the steady-state as a function of the current mean m (markers), for increasing values of the fluctuation amplitude s, and compared to the corresponding model best-fit prediction (lines). (Modified and reproduced with permission, © 2004, The American Physiological Society.)

respond as simple integrate-and-fire (IF) units (Figure 10.7; Giugliano et al., 2004). Actually, the curves $f(m,s^2)$, collected for each cell at the steady-state, are reproduced with high accuracy by the response function $\Phi(m,s^2)$ of an identified IF model (see Equation (10.2) and Appendix). This proves that the biophysical and morphological details of a neuron collapse into an extremely simplified quantitative description of neuronal integration and excitability, when studied under appropriate realistic conditions.

10.4.1 Leaky Integrate-and-Fire Model

A single-compartment description of neuronal excitability was therefore enough to account for the entire experimental data set. This is surprising, as the model relies on a very small number of free parameters (i.e., 5), which were identified in each experiment by numerical optimization techniques. Such a model is known as the Lapicque's or leaky IF (Tuckwell, 1988) and it has been extensively studied (Fourcaud and Brunel, 2002, Mattia and Del Giudice, 2002) and employed in

large-scale network simulations (Reutimann et al., 2003). As opposed to biophysically realistic models (Abbott and Dayan, 2001), the leaky IF is characterized just by a single state-variable V, representing the membrane potential, and by a reduced set of effective constant parameters, as follows.

$$\mathrm{C}\,\frac{\mathrm{dV(t)}}{\mathrm{dt}} = \begin{cases} \bar{\mathrm{g}}\,(\mathrm{E}-\mathrm{V}) + \mathrm{I_m(t)} & \text{if } \mathrm{V(t)} < \vartheta \\ 0,\ \mathrm{V(t)} = \mathrm{H} & \text{if } \mathrm{V(E_0)} = \vartheta \text{ and } \mathrm{t} \in (\mathrm{t_0};\, \mathrm{t_0} + \tau_{\mathrm{arp}}) \end{cases} \tag{10.2}$$

In the previous definition, the absolute refractory period and hyperpolarization voltage following the emission of an action potential have been indicated by τ_{arp} and H, respectively. Moreover, the integration operated by the neuronal membrane is assumed to be passive and characterized by a voltage-independent ionic conductance (g) and by a capacitance C. All the nonlinearities associated with the emission of an action potential (Hodgkin and Huxley, 1952), have been lumped into a fixed voltage threshold ϑ, therefore describing each spike as a highly stereotyped event that corresponds to a threshold crossing for V (see Appendix). Finally, below threshold, the membrane voltage decays to its resting value E, when the total membrane current $I_m(t) = 0$.

10.4.2 Spike-Frequency Adaptation and Slow/Cumulative Inactivation

In all the noisy current-clamp experiments, the temporal dynamics of the instantaneous output firing rate $f = f(t)$ was characterized by fast and frequency-dependent adaptation components, which occur over a time scale of several hundred milliseconds, and by a slower component, occurring over a time scale of several seconds (Sanchez-Vives et al., 2000; Powers et al., 1999; Sawczuk et al., 1997; Fleidervish et al., 1996; Douglas and Martin, 1990). These mechanisms, together with homosynaptic depression (Tsodyks et al., 2000), have been proposed as candidates for the generation of oscillatory activities in the nervous system, and related to the termination of the PB (Giugliano et al., 2004; van Vreeswijk and Hansel, 2001). In order to account for the single-cell experimental recordings, the IF model further incorporated a simplified adaptation current, describing the contribution of intracellular calcium- and/or sodium-activated outward currents. $I_m(t)$ was therefore identified as the sum of an intrinsic contribution $I_X(t)$, due to adaptation mechanisms, and an external/synaptic current $I(t)$. Each emitted spike was then assumed to cause a sudden increase in the intracellular concentration $X(t)$ of the ions, involved in such an activity-dependent hyperpolarization current, which was formalized as follows.

$$\begin{aligned} \mathrm{I_X(t)} &= -\alpha \mathrm{X(t)} \\ \tau_{\mathrm{a}} \frac{\mathrm{dX(t)}}{\mathrm{dt}} &= -\mathrm{X(t)},\ \mathrm{X}(\mathrm{t}_0^+) \rightarrow \mathrm{X}(\mathrm{t}_0^-) + \tau_{\mathrm{a}}^{-1} \end{aligned} \tag{10.3}$$

The stationary effect of fast and slow adaptation processes at steady-state was therefore captured by this simple mechanism, and it reduced the slope of the curve $\Phi(m,s^2)$ by the factor α (see Appendix).

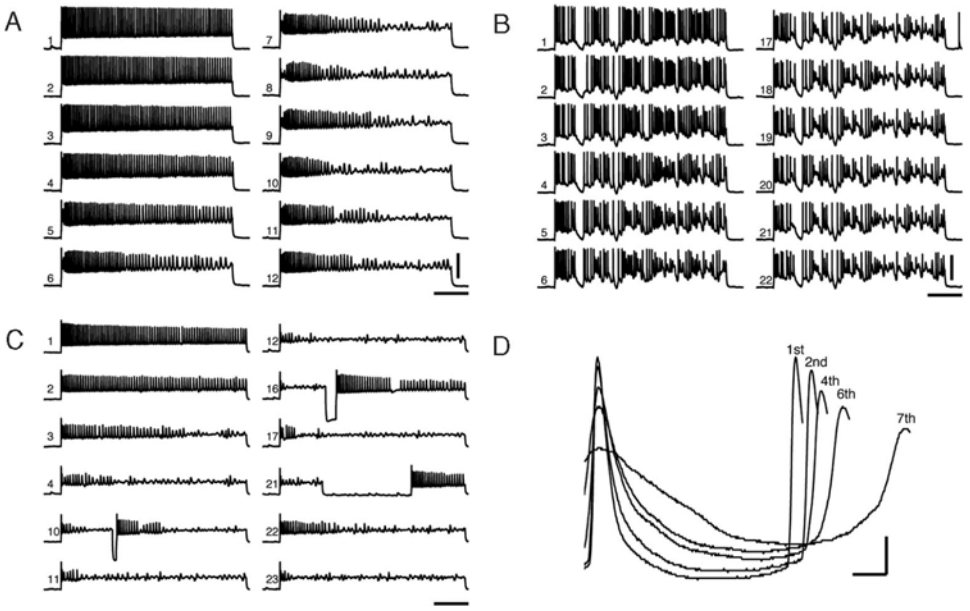

FIGURE 10.8. Slow inactivation of spike-generation mechanisms. Inactivation contributes to determine the maximal steady-state spike frequency that cortical neurons are able to sustain. Similarly to the effect of sodium/calcium-dependent potassium currents, such an inactivation might participate in the termination of each population burst. A repeated intracellular DC current stimulation (A), with very short interstimulus pauses, makes the spike inactivation apparent. Such an inactivation slowly builds in time, and increasingly affects (D) the amplitude, the interspike intervals, and the maximal upstroke velocity of successive action potentials. (B) The same phenomenon affects neuronal responses under noisy current-clamp. However, the voltage fluctuations, induced by the nondeterministic current component, may delay the expression of inactivation, and transiently reverse it. (C) The cumulative character of such a slow inactivation can be revealed by delivering short hyperpolarizing current pulses, interleaved to DC current stimuli: inactivation can be reversed only partially (calibration: 1 sec/50 mV for (A–C); 10 msec/10 mV for (D)).

However, an additional cumulative component, related to the inactivation of the spike generation mechanisms, characterized neuronal responses (see Figure 10.8). The presence of such cumulative inactivation was explicitly tested by extending the protocol described in Fleidervish et al. (1996) and Schwindt et al. (1989), which consists in a repeated pulse-stimulation lasting 1 sec, with a very short recovery time. Under noisy current injection, and employing the same current realization for each repetition, the same phenomenon occurred, although the voltage fluctuations, induced by the nondeterministic stimulus waveform, could delay the onset of inactivation at parity of m, and sometimes transiently reversed the inactivation for a few tens of milliseconds, as compared to DC stimuli. For the sake of simplicity, such an intrinsic inactivation was not considered in the IF model (but see Giugliano et al., 2002).

10.4.3 A Simple Model of Chemical Synaptic Interactions

Although we did not experimentally approach the effective characterization of synaptic physiology so far, there are enough data available from the literature to define a minimal model of chemical synaptic interactions between cortical neurons in vitro (see also Giugliano (2000)). Consistent with the hypotheses underlying the current stimuli injected in single-neuron experiments, synaptic coupling is described by current rather than conductance changes (see La Camera et al. (2003) for a discussion). Interactions between any two connected neurons are triggered by presynaptic emission of an action potential, after an effective delay δ of 1.5 msec, which includes the axonal delay and the synaptic release latency (Nakanishi and Kukita, 1998). Each postsynaptic current consists of an instantaneous rise to J_e (i.e., the synaptic efficacy) and by an exponential decay with a time constant $\tau_e = 5$ msec (see Figure 10.3). In the case of a population of N_e excitatory neurons, the total synaptic current $I_i(t)$ into the neuron i is therefore given by:

$$\mathrm{I_i(t)} = \sum_{\mathrm{j=1}}^{\mathrm{N_e}} \sum_{\mathrm{k}} \mathrm{J_e C_{ij}}\ \mathrm{e}^{-(\mathrm{t}-\mathrm{t}_\mathrm{k}^\mathrm{j}-\delta)/\tau_\mathrm{e}} \Theta(\mathrm{t}-\mathrm{t}_\mathrm{k}^\mathrm{j}-\delta) \tag{10.4}$$

where $\{t_k^j\}$ are the times of emission of action potentials by the jth presynaptic neuron, C_{ij} is the connectivity matrix, and $\Theta(t)$ is the step function (i.e., $\Theta(t) = 0$, $t < 0$ and $\Theta(t) = 1$, $t \geq 0$). The probability of connection (i.e., $C_{ij} = 1$) was fixed to 0.3 to 0.4 (Nakanishi and Kukita, 1998), and the effect of spontaneous synaptic release and of other sources of randomness (Maeda et al., 1995) was incorporated as an activity-independent additional irregular synaptic drive (Giugliano et al., 2004).

10.5 A Network of IF Model Neurons

The results presented and briefly discussed in previous sections indicate that an extremely simple mathematical model of neuronal electrical activity can be employed to describe the discharge properties of individual dissociated neocortical neurons cultured in vitro. Moreover, the experiments performed by patch-clamp allowed us to identify the numerical parameters of such a description. Thus, such effective values can be immediately incorporated in a model of a network of synaptically connected IF neurons, to be studied and computer simulated with unparalleled realism. We approached the study of such a model network in two ways: by direct numerical simulation and by mean field theoretical analysis. For the sake of simplicity, we focus on the electrical activity of a homogeneous population composed only of excitatory model neurons. With the aim of comparing model performances to real MEA data, we consider a set of experiments obtained in the presence of bicuculline, a blocker of GABA_A inhibitory synaptic receptors (see Figure 10.9).

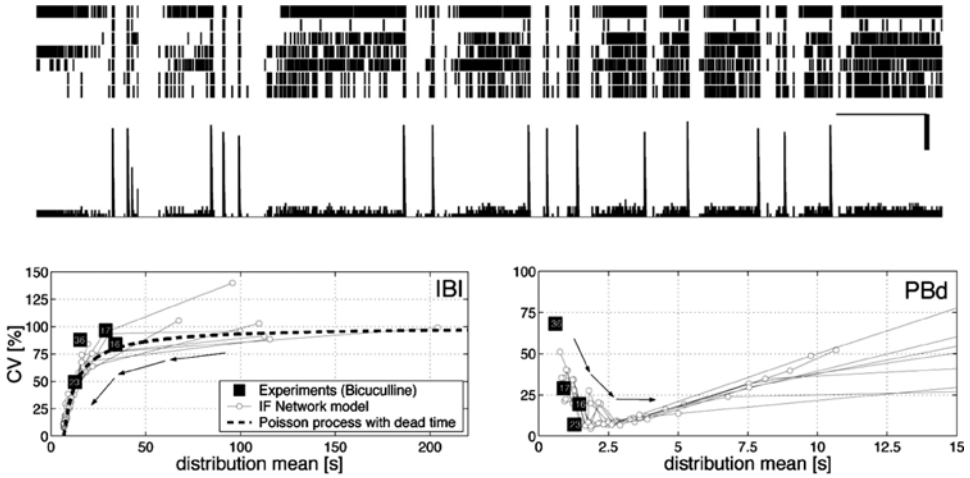

FIGURE 10.9. Network activity emerging in dissociated cultures of neocortical neurons, detected by MEAs. The raster plot (upper panels) indicates the time of occurrence of the events extracellularly detected by 7 substrate electrodes, and below the resulting population mean firing rate is reported (scale bars: 60 sec, 10 Hz). To compare the performances of computer simulations to real network data, results from 4 MEA experiments in the presence of bicuculline were considered, by simultaneously studying (lower panels) the coefficient of variation (CV), and the mean of the interbursts intervals (IBIs) distribution, and of the duration of the population bursts (PBd). Numbers associated with each marker help to identify the same experiment in both plots and indicate the number of PBs, collected over 10 min of continuous recording. Computer simulations of the network of *IF* model neurons reproduced the same features of the spontaneous patterned activity, simultaneously matching the IBIs and the PBd, for increasing values of synaptic coupling. (Indicated by the arrows; modified and reproduced with permission, © 2004, The American Physiological Society.)

10.5.1 Computer Numerical Simulations

The numerical simulation of the network model described above consists in the simultaneous integration of Equations (10.2) through (10.4), for each neuron of the network (Giugliano et al., 2004), by an appropriate discrete-time algorithm implemented on a desktop computer (see, for instance, Reutimann et al. (2003)). To our surprise, as soon as we incorporated the features and parameters estimated from the experiments into the model, spontaneous electrical activity arose and organized into a population bursting. Although individual IF neurons of the simulated network are not intrinsic burster cells (Smith et al., 2000; McCormick et al., 1985), and no pacemaker mechanism had been explicitly introduced and localized in the model, we assisted in the emergence of a repetitive transient networkwide synchronization of electrical activity, strikingly similar to what we measured in a real network of cortical cells cultured over the MEAs (see Figure 10.9, upper panel).

In these simulations, the spatial origin of the PBs varies randomly with each PB, consistent with the lack of spatial structure in the network and with the

(experimental) conclusions about the lack of a unique rhythm generator mechanism driving the network. As several investigators noted the regular/irregular character of PBs (Wiedemann and Lüthi, 2003; Nakanishi et al., 2001; Maeda et al., 1995), we took a careful look at the features of activity in our model. This is quite relevant as the highly irregular character of neuronal firing is ubiquitous in in vivo cortical physiology (Destexhe et al., 2003; Shadlen and Newsome, 1998). We found that the frequency and the character of the simulated PBs depended strongly on the synaptic connectivity and on the excitatory coupling J_e. In particular, by increasing J_e, we indeed observed three different regimes: asynchronous irregular firing, periodic synchronized bursting, and nonperiodic synchronized bursting.

First of all, in order to model a condition of very weak excitatory coupling between neurons, or to mimic a very low connectivity, we set J_e very small. Under such conditions, the network of model neurons is characterized by low-rate asynchronous spiking activity. Such a background activity is mainly determined by activity-independent synaptic activation and only weakly by the contribution of recurrent connections. No spontaneous PB occurs and any brief depolarizing stimulus, even delivered to a large fraction of neurons of the network, does not evoke spiking activity that persists more than the duration of the stimulus.

In terms of a theoretical interpretation that is discussed in the following sections, we may conclude that under such conditions, the dynamics of the whole population is dominated by a single low-rate stable state, as the recurrent synaptic feedback is too weak to self-sustain a reverberating activity. We should note that, in our model, the reliability of synaptic transmission remains unchanged and does not "mature" with time (see Equation (10.4)). Anyway, at low firing rates, low values of J_e can also statistically account for low-probability synaptic release, characterizing immature synapses (Tsodyks et al., 2000; Kamioka et al., 1996). As discussed at the beginning of this chapter, such a situation approximates the early developmental stage of cultured networks.

In another set of computer simulations, we substantially increased J_e. A larger value of J_e may correspond to an increase in both the number and efficacy of synaptic contacts, as observed in vitro during maturation (Muramoto et al., 1993). Under such conditions, where the low-rate random spiking is still present and at the same frequency, spontaneous PBs occur very frequently and regularly. Now, even a brief external triggering stimulus successfully recruits neurons to produce evoked PBs, whose duration is inversely determined by α, and independent of stimulus strength.

Actually, in such a regime the global dynamics of the network is transiently bistable: once a PB is started, adaptation slowly redefines the location and existence of the network stable states, until there is suddenly only a single stable state at 0 Hz, similarly to what is observed after each PB in the MEA experiments (see Figure 10.9, upper panel). In details, the adaptation hyperpolarizing currents $I_X(t)$, which start to build up in every neuron recruited by a PB (see Equation (10.3)), decrease the mean input current and therefore lower the output firing rate (see Figure 10.7), until the recurrent synaptic inputs stop. This may be considered as a kind of reset for the collective network activity. Later, the network is refractory

as the mechanisms of spike-frequency adaptation recover (i.e., $X(t) \to 0$), for a time that is proportional to τ_a. In particular, we note that although the value of τ_a can be estimated from the transient time course of $f(t)$, upon current stimulation, it is feasible that its actual value changes due to the degree of network maturation.

Finally, for very strong synaptic coupling, the network loses its bistable transient properties, and only a high-frequency firing characterizes the network. We doubt that such a regime can be directly observed in vitro, because of the impact of additional adaptation mechanisms (Figure 10.8), and because of other metabolic constraints on neuronal firing (e.g., the activity of ATP-operated electrogenic pumps). These processes act on a very long time scale, compared to a single spike, and they would switch off network activity by down-regulating intrinsic neuronal excitability (i.e., changing the profile of Φ_{IF}). Such a scenario would probably result in a synchronized bursting with very long burst-recovery intervals, and it would not be always possible to evoke a PB by electrical stimulation, during the spontaneous interburst intervals (Kamioka et al., 1996).

10.5.2 Theory

In the case of the network architecture discussed here, the statistics of the total synaptic current received by a generic neuron are described by the following recurrent mean field equations,

$$\mathrm{m(f)} = \mathrm{N_e C_{ee} J_e f \tau_e} + \mathrm{m_0} \text{ and } \mathrm{s^2(f)} = \mathrm{N_e\ C_{ee}\, J_e^2\, f\, \tau_e/2} + \mathrm{s_0^2}, \tag{10.5}$$

where f is the network mean firing rate and J_e the effective peak-amplitude for the individual postsynaptic currents. By m_0 and s_0^2, we indicate two fixed parameters, corresponding to the spontaneous neurotransmitter release and other sources of randomness, independent of f by hypothesis.

As mentioned in the previous sections, the knowledge of the single-neuron response function $f(m,s^2)$, identified in the experiments, lets us derive quantitative predictions and interpretations on the collective network properties. This is possible, under the same extended mean-field hypotheses that underlie the noisy currents (Equation (10.1)), injected into real neurons, and it can be done without running a single numerical simulation.

In fact, an in vitro network of synaptically interacting excitatory neurons may be regarded as a single dynamical system. Its stationary states can be predicted and interpreted, in the limit of an infinite number of neurons $N_e \to \infty$, by employing the mean-field equations (10.5) and studying $\Phi_{IF}(m(f), s(f))$ as a function of f (Amit and Brunel, 1997), in particular looking for its fixed points.

For the sake of clarity, we first consider the collective activity in the absence of spike-frequency dependent adaptation (i.e., $\alpha = 0$). Because of the simultaneous dependence of Φ_{IF} on m and s^2, the collective firing-rate of the network may be characterized by two stable dynamic-equilibrium states, in a range of synaptic coupling J_e (see Figures 10.10A and 10.11A). Such global activity configurations correspond to the solutions f^* of the following self-consistent network equation,

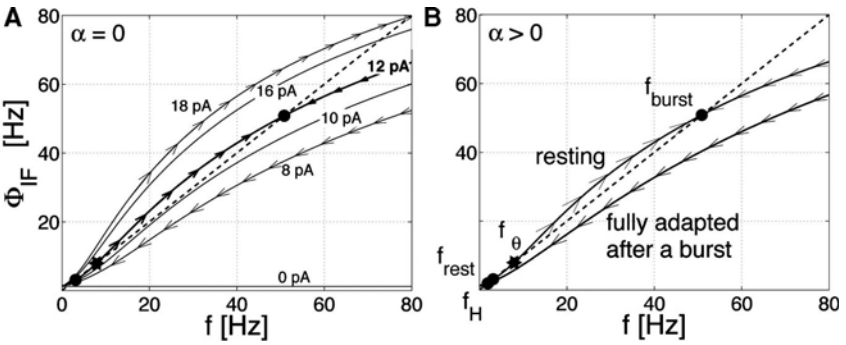

FIGURE 10.10. Prediction of the collective activity emerging in a homogeneous population of excitatory neurons based on single-neuron response properties. (A) The plot represents the profile of $\Phi_{\mathrm{IF}}(m(f), s^2(f))$ as a function of network firing rate f, for increasing values of the average synaptic efficacy J_e. In a small range of synaptic coupling, the network may be characterized by two distinct dynamic-equilibrium states for the collective activity ($\alpha = 0$, circles: stable states; star: unstable state). (B) Φ_{IF} was then plotted as a function of f, while comparing the instantaneous network response profile immediately before a PB (resting) and after the complete buildup of adaptation currents I_X, at the end of the same PB (fully adapted). When the network is active at a low frequency regime f_{rest}, the impact of the spike-frequency dependent adaptation is negligible and an additional equilibrium stable state, at a high frequency f_{burst}, may characterize the collective dynamics. However, if a transition $f_{\mathrm{rest}} \rightarrow f_{\mathrm{burst}}$ occurs, the adaptation starts to slowly build up, bending the network response profile until no stable dynamic equilibrium state at high frequency can be sustained anymore ($f(t) \rightarrow f_H$). Thus, it can be inferred that the actual network mean firing rate will be flipping between two states, in an alternating and activity-dependent way, as confirmed by computer simulations (see Figures 10.9 and 10.11). (Modified and reproduced with permission, © 2004, The American Physiological Society.)

further satisfying a stability condition:

$$\mathrm{f}^* = \Phi_{\mathrm{IF}}(\mathrm{m}(\mathrm{f}^*), \mathrm{s}(\mathrm{f}^*)) \quad \frac{\mathrm{d}}{\mathrm{df}}\Phi_{\mathrm{IF}}(\mathrm{f}^*) < 1.$$

These solutions have been graphically identified as the intersection points of $\Phi_{IF}(f)$ with the unitary-slope line, and marked as circles (stable) and stars (unstable states) (see Figure 10.10A).

When occupying a stable dynamic regime, the activity of the network is the result of the interactions between the neurons, and a transition from one state to the other can occur spontaneously in small networks. Actually, these transitions might be the result of fluctuations induced by finite-size effects (Mattia and Del Giudice, 2002), or they can be triggered by an external brief stimulus (Figure 10.11).

10.5.3 Mechanisms of PB

Considering the full network model, where individual neurons keep adapting their output rate as a function of activity (i.e., $\langle X(t) \rangle \sim f(t)$), it is possible to carry

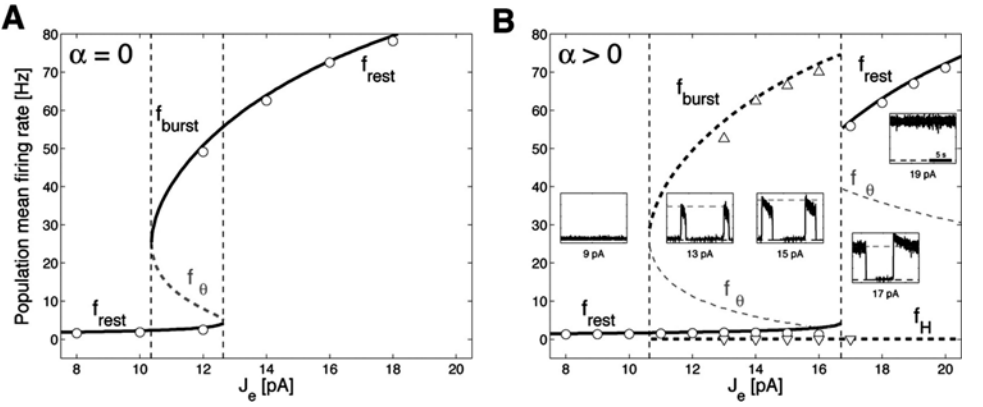

FIGURE 10.11. Network bistability in the absence of adaptation and other sources of non-stationarity in a homogeneous excitatory population, for a small range of synaptic coupling J_e (A). This is a direct consequence of the profile of the network response function, experimentally characterized in Figure 10.7. A similar phase diagram can be considered for the model network, including adaptation (B). By studying the quasi-stationary/instantaneous stable states, it is possible to make quantitative predictions on the mean firing rates during asynchronous regimes as well as during population bursts. The insets report the actual traces of simulated network activity for different synaptic coupling, and compare the actual resting and bursting activity levels with the predictions of the theory (black and gray dotted lines). In both panels, black continuous and dashed traces indicate stationary and quasi-stationary stable states, respectively. Dashed gray lines report the location of unstable stationary and quasi-stationary equilibria, whose distance from f_{rest} determines the regular/irregular character of network oscillations. The markers represent the network mean firing rates, measured in computer simulations under different regimes. Although the simulated network considered was very small, $N_e = 100$, the agreement between theoretical predictions and numerical computer simulations is remarkable. (Reproduced with permission, © 2004, The American Physiological Society.)

out an approximate analysis. Provided that the mechanisms responsible for the reduction of excitability (e.g., adaptation) act on a time scale (τ_a), much longer than the single-neuron dynamics ($c/\bar{g}$), an analysis of the quasi-stationary equilibria may be representative of the collective activity of the network. In other words, by assuming that adaptation is delayed and transiently uncoupled from intrinsic neuronal dynamics, we may consider it as frozen and determined by the previous global conditions.

Let's consider the situation of small J_e: a low-rate stable regime f_{rest} is expected to characterize the network dynamics, as it can be immediately determined from Φ_{IF}. By making explicit the dependence on α (see Equation (10.5) and Appendix), we can write the following self-consistent equation and solve it to find the stable solution f_{rest},

$$f_{\text{rest}} = \Phi_{\text{IF}}(m(f_{\text{rest}}) - \alpha f_{\text{rest}}, s(f_{\text{rest}})).$$

As confirmed by computer simulations, the instantaneous network firing rate $f(t)$ fluctuates around f_{rest}, as a result of finite-size network effects. However, each neuron of the network instantaneously responds to its input drive according to a quasi-stationary input–output response function given by

$$\Phi_{IF}(m - \alpha\, f_{\text{rest}}, s),$$

with f_{rest} a constant. Neurons are therefore not experiencing immediately the impact of adaptation. Thus, let's assume that the network *was* at "rest". We may now determine the existence of any additional stable dynamical attractor f^*. f^* must satisfy the following equation,

$$f^* = \Phi_{IF}(m(f^*) - \alpha\, f_{\text{rest}},\ s(f^*)).$$

$f^* = f_{\text{rest}}$ is of course a solution of the previous equation, but for increasing values of J_e, $f^* = f_{\text{burst}}$ is also a solution ($f_{\text{burst}} > f_{\text{rest}}$, Figure 10.10B). Under these circumstances there always exists an intermediate unstable equilibrium f'_θ ($f_{\text{rest}} < f'_\theta < f_{\text{burst}}$), satisfying the previous relationship and separating the two basins of attraction (Figure 10.10B).

Intuitively, when a fluctuation in the global activity of a "resting" network is large enough to overcome the distance $\Delta'_\theta = (f'_\theta - f_{\text{rest}})$, the stability of f_{rest} may be (transiently) lost and the entire network synchronously shifts to a new regime where $f(t) = f_{\text{burst}}$. The unstable state is therefore acting as a no-return point, similarly to what happens to the membrane voltage of a neuron during the generation of an action-potential.

Anyway, such a regime cannot be sustained indefinitely, because f_{burst} is not a solution of the full, self-consistent equation, including the *updated* effects of adaptation

$$f^* = \Phi_{IF}(m(f^*) - \alpha\, f_{\text{burst}}, s(f^*)).$$

Instead, such an equation is satisfied by $f^* = f_H \approx 0$ Hz, with $f_H < f_{\text{burst}}$ (see Figure 10.10B). Therefore, although adaptation progressively builds up in individual neurons, network activity decreases and the locations of the f_{burst} and f'_θ tend to approach and finally overlap, until their existence is suddenly lost (see Figure 10.10B). When this occurs, the network dynamics suddenly converges to f_H and most neurons stop firing, similarly to the hyperpolarization experienced by the membrane voltage after an action-potential. This accounts quantitatively for the generation of PBs, as compared to direct network simulations (Figure 10.11B, markers). By analogy, the amount of time spent in PB is therefore related to the distance $\Delta' = (f_{\text{burst}} - f'_\theta)$ and to the time requested by adaptation for the full buildup (i.e., α and τ_a). Qualitatively, it can be concluded that for an increasing J_e, Δ'_θ decreases whereas Δ' increases, thus the mean interburst interval (IBI) decreases and the mean duration of PB (PBd) increases.

Finally, as in the previous case, such a new regime cannot be sustained indefinitely, because f_H is not a solution of:

$$f^* = \Phi_{IF}(m(f^*) - \alpha\, f_H, s(f^*)).$$

The network will thus recover its resting activity level $f_{\text{rest}} > f_H$, as described at the beginning.

10.5.4 Variability of the IBIs Distribution

From the considerations developed so far, it is possible to interpret the regular/irregular character of the IBIs. In the last paragraphs, an analogy between PBs and action potentials occurring in an excitable membrane was often proposed and it is now exploited. In fact, similarly to the temporal evolution of the membrane potential in the single-neuron IF dynamics, the activity of a network randomly fluctuates as a result of synaptic noise. Occasionally, these fluctuations may be large enough to overcome an excitability threshold (i.e., Δ'_θ). When this happens, a major explosive event occurs ($f \to f_{\text{burst}}$), and later the activity is strongly refractory to any further generation of PBs ($f \approx f_H$). The generation of PBs is somehow similar to the generation of an action potential in a model of integration of a noisy input. By mapping the population mean firing rate f into the membrane voltage of an abstract IF model neuron, we make the previous comparisons explicit, setting the resting membrane voltage to f_{rest}, the spike threshold to f'_θ, the reset potential to f_H, and the absolute refractory period proportional to τ_a.

An increase in network synaptic coupling J_e induces a decrease in the distance $f'_\theta - f_{\text{rest}}$ (see Figure 10.11B), so that the rate of threshold crossing is expected to monotonically increase, while preserving an irregular character. Such predictions were confirmed by the simulated network activity, where IBIs statistics are approximated by a Poisson process with a refractory time (see Figure 10.9, lower panel, dotted thick line). This is reminiscent of a widely studied balanced (i.e., drift-free) integration process (see Shadlen and Newsome (1998)), where the threshold crossings are determined by subthreshold fluctuations only, in a noise-dominated regime.

10.5.5 Interpreting MEA Experimental Data

As anticipated, we conclude that the frequency and regular/irregular character of spontaneous population bursting are intimately related to the synaptic strength J_e, and inversely, on the size of the network. The last dependence is associated with the amplitude of random fluctuations in the population firing rate, which are produced by finite-size network effects (Mattia and Del Giudice, 2002). At a parity of network size, we predict and observe a rare and unpredictable occurrence of short and irregular PBs, for intermediate values of J_e, and a frequent and more regular occurrence of longer and more regular PBs, for larger J_e.

Here, we attempt to provide an interpretation of the MEA experiments, consistent with the insights gained from the theory. This brings us to conclude that around 1 to 5 DIV, because the number and effectiveness of in vitro synapses are very low (i.e., J_e is small), no PB can occur because the network is intrinsically incapable of self-sustaining (transient) reverberating activity of a PB. Later, the strong neuritic outgrowth and synaptogenesis turn the network into a bistable device. We speculate

that such conditions may correspond to an overshoot phase of in vitro network development, consisting in an over-expression of branches and synaptic boutons, resulting in a large J_e. As described in the previous subsection, the recurrent connections of the network can now transiently sustain a regular population bursting, mainly determined and dominated by the recovery time constants of intrinsic neuronal adaptation. Later, as the network reaches its mature condition, pruning of a large fraction of synaptic contacts, or modulation of synaptic efficacy by homeostatic processes (see Figure 10.2), makes J_e substantially smaller. In such a regime, the statistics of the simulated IBIs and PBd matched the results of the MEA experiments, performed under pharmacological disinhibition (see Figure 10.9).

We propose the diagram of Figure 10.11 to summarize the prediction of the theory, as well as the results of the computer simulation. Any pharmacological and/or ionic manipulation of excitatory synaptic efficacy is expected to alter not only the frequency and the regular/irregular occurrence of PBs, but also the interburst spiking frequency, according to the trajectory indicated by triangles and the dotted thick line of Figure 10.11B.

Lowering extracellular magnesium concentration, by increasing activation of NMDA-receptors, is expected to unveil population bursting in a silent mature culture (Robinson et al., 1993). Similarly, a decrease in the concentration of extracellular calcium ions would tend first to drive a regularly bursting mature network into a rare unpredictable bursting regime, and finally to abolish completely each PB (Canepari et al., 1997). Therefore, the action of bath-applied drugs such as AP-V, CNQX, cyclothiazide, or the modulation of extracellular ions such as Mg^{++} and Ca^{++}, largely involved in excitatory synaptic transmission, can be roughly mapped as modulations of J_e. The outcome of such a modulation depends of course on the intensity and sign of these manipulations, as well as on the previous state of the network (Turrigiano and Nelson, 2004).

From the phase diagram of Figure 10.11, it becomes clear that by a partial blockade of glutamatergic synaptic receptors, PBs disappear whereas asynchronous isolated spiking activity may persist (Kamioka et al., 1996). A complete blockade of synaptic transmission would remove also the background random activity, as neurons become insensitive to the fluctuations induced by spontaneous synaptic release (i.e., $m_0 = s_0 = 0$).

A final prediction of this theory consists in the monotonic dependence on J_e of the interburst firing rate (Nakanishi and Kukita, 1998; Maeda et al., 1998; Canepari et al., 1997; Kamioka et al., 1996). The use of repeated extracellular stimulation known to induce activity-dependent potentiation of synaptic efficacy in a long-term manner, and corresponding to an increase in J_e, is expected to: (i) turn a previously spontaneously silent mature network into an active one by increasing the probability of spontaneous PBs; (ii) turn a silent network, previously nonresponsive to electrical stimulation, into a system that generates a PB upon electrical stimulation; and (iii) increase the number of bursts per minute, while increasing the number of spikes per burst (Maeda et al., 1998). Finally, a graded modulation of synaptic efficacy J_e is expected to induce a graded modification on the network dynamics (Maeda et al., 1998).

10.6 Concluding Remarks

In vivo cortical processing naturally arises from interconnections among large populations of neurons and simultaneous feedback from several brain structures. Such conditions are of course completely lacking in isolated brain slices and cell cultures. Nevertheless, approaching the in vitro network level from the knowledge of single neurons and synapses, understanding how much complexity is the result of the interactions and how much is intrinsic, does represent a powerful tool to challenge our models and predictions on small-scale reduced problems.

In this chapter, single-neuron discharge properties have been investigated in dissociated cultures of neocortex coupled to MEAs, demonstrating that a simplified point-neuron IF model is an adequate description when network mean firing rates are considered. It is significant that spike response properties of cultured neocortical neurons qualitatively resemble those of cells in acute slice preparations. This is of great importance as dissociated neurons might undergo a different ex vivo development of intrinsic biophysical properties.

The same patterned activity, experimentally characterized in vitro by MEA recordings, was reproduced in the simulated networks, and interpreted in terms of the network-response properties, emerging from $f = \Phi(m,s)$. Matching with MEA recordings is satisfactory, indicating that the discharge response properties to noisy current stimuli and the experimentally characterized spike-frequency adaptation are indeed sufficient to account for the emerging collective activity, observed in the experiments. Finally, it is interesting to note that the reduction driven by the experimental data at the single-neuron level did not compromise the richness of phenomena occurring at the level of a population.

Acknowledgments. The authors thank Stefano Fusi, Giancarlo La Camera, and Anne Tscherter for helpful discussions, and Ruth Rubli for assistance. This work was supported by the Swiss National Science Foundation, the Human Frontier Science Program, the EC Thematic Network in Neuroinformatics and Computational Neuroscience, and the University of Genova, Italy.

Appendix A

A.1 The Membrane Potential as a Diffusion Process

In order to characterize the spiking response of an IF model neuron under noisy current inputs, it is convenient to normalize all voltages to the resting membrane voltage E, and to introduce the probability density function $P_V(v,t)$ (Fourcaud and Brunel, 2002; Fusi and Mattia, 1999; Abeles, 1991). Such a function gives at any time t the probability that the membrane voltage $V(t)$ approaches values around v:

$$P_V(v,t)\,dv = \text{Prob}\{v < V(t) \leq v + dv\}. \tag{A.1}$$

Such a characterization accounts for the trajectories of the membrane potential, resulting from any possible current input. In a generalized IF model, with a state- and time-dependent intrinsic membrane current $L(V, t)$ (Fourcaud-Trocmé et al., 2003), the membrane potential evolves subthreshold as

$$C\frac{dV}{dt} = L(V, t) + I(t). \tag{A.2}$$

When $I(t)$ is a delta-correlated and Gauss-distributed process, with infinitesimal mean and variance μ and σ^2, respectively, $V(t)$ is a stochastic diffusion process. As a consequence, the probability density $P_V(v, t)$ satisfies an equation known as the Fokker–Planck equation (Fourcaud and Brunel, 2002; Risken, 1984; Cox and Miller, 1965):

$$\frac{\partial}{\partial t}\ P_V(v, t) = -\frac{\partial}{\partial v}\ \phi(v, t). \tag{A.3}$$

In the previous equation, the right-hand side is reminiscent of the gradient of a flux of particles in a diffusion equation, and it can be identified as the sum of a diffusive term and a drift-related term:

$$\phi(v, t) = -\frac{\sigma^2}{2}\frac{\partial}{\partial v}\ P_V(v, t) + (\mu - L(V, t))\ P_V(v, t). \tag{A.4}$$

Readers interested in the derivation of Equation (A.3), may refer to the literature (Risken, 1984; Cox and Miller, 1965).

A.2 The Current-to-Rate Response Function

By analogy with the diffusion of a substance in a medium, it is possible to identify and evaluate the neuron spiking mean rate $f(t)$ at time t, as the number of first-passages $V(t) = \vartheta$, in the time unit. This coincides with the definition of the flux ϕ at the spike-threshold, because of the additional boundary conditions that must satisfy Equation (A.3) (see below):

$$f(t) = \phi(\vartheta, t) \tag{A.5}$$

At steady-state, such a quantity has been defined as the current-to-rate response function (Tuckwell, 1988; Ricciardi, 1977); it was estimated experimentally in rat neocortical neurons (Giugliano et al., 2004; Rauch et al., 2003) and indicated by $\Phi_{\mathrm{IF}}(\mu,\ \sigma^2)$ as a function of the input current statistics.

As anticipated, appropriate boundary conditions must be specified to introduce the nonlinearities of the IF dynamics (see also Fusi and Mattia, 1999). These are related to the excitability threshold ϑ, the reset potential H, and the refractory period τ_{arp}. The analogy with a process of diffusion in a medium can be pursued identifying $P_V(v, t)$ as an instantaneous concentration, and discussing the way it is restricted.

- At $V = \vartheta$, in terms of an absorbing barrier, because the particles (i.e., neurons) that are crossing such a threshold are "absorbed" at any time, and leave the

interval $(-\infty; \vartheta)$ to undergo refractoriness:

$$\forall t,\ P_V(\vartheta, t) = 0 \tag{A.6}$$

- At $V = H$, in terms of a discontinuity in the flux $\phi(H, t)$, due to the spike-reset mechanisms and the consequent flow of previously absorbed particles, coming out from refractoriness:

$$\lim_{\varepsilon \to 0} \left(\phi(H + \varepsilon, t) - \phi(H - \varepsilon, t)\right) = f(t - \tau_{\text{arp}}) \tag{A.7}$$

At any time t, $P_V(v, t)$ must further satisfy a normalization condition

$$\int_{-\infty}^{\vartheta} P_V(v, t)\, dv + \int_{t}^{t+\tau_{\text{arp}}} f(t')\, dt' = 1, \tag{A.8}$$

because no neuron is allowed to have a membrane potential outside the range $(-\infty; \vartheta)$, unless it is refractory (i.e., no "particle" is destroyed or generated).

For the leaky IF (Equation (A.2)), we finally report the expression of the current-to-frequency response function at the steady-state (Ricciardi, 1977), which can be derived from Equations (A.3), and (A.6) through (A.8), by setting $L(V, t) = \bar{g}V$ and dropping any temporal dependence:

$$f = \phi(\vartheta) = \Phi = \left[\tau_{\text{arp}} + \tau\sqrt{\pi} \int_{(\hat{H})}^{(\hat{\vartheta})} e^{x^2}(1 + erf(x))\, dx\right]^{-1} \tag{A.9}$$

where $\tau = C/\bar{g}$ is the neuron membrane time constant, *erf*(x) indicates the error function (Abramowitz and Stegun, 1994), and

$$\hat{H} = (H - \mu\tau)/(\sigma\sqrt{\tau}),\ \hat{\vartheta} = (\vartheta - \mu\tau)/(\sigma\sqrt{\tau}),$$
$$\mu = m/C,\ \sigma = (s\sqrt{2\tau_1})/C.$$

We note that the current-to-frequency response function, employed for the fit of experimental data curves (see Figure 10.7), incorporated the stationary effect of the adaptation current $I_X(t)$ (see also Equation (A.3)). This is reintroduced by replacing m with $(m - \alpha f)$ in the previous expressions, obtaining an implicit expression to be solved in f. In fact, adaptation currents affect only the steady-state mean current without changing substantially the input variance (La Camera et al., 2002).

References

Abbott, L.F. and Dayan, P. (2001). *Theoretical Neuroscience*. MIT Press, Cambridge.

Abeles, M. (1991). Relations between membrane potential and the synaptic response curve. In *Corticonics: Neural Circuits of the Cerebral Cortex*, Cambridge University Press, Cambridge, UK, Chap. 4, pp. 118–149.

Abramowitz, M. and Stegun, I.A. (1994). *Tables of Mathematical Functions*. Dover, New York.

Amit, D.J. (1989). *Modeling Brain Function*. Cambridge University Press, Cambridge, UK.

Amit, D.J. and Brunel, N. (1997). Model of global spontaneous activity and local structured (learned) delay activity during delay. *Cerebral Cortex* 7: 237–252.

Bove, M., Martinoia, S., Verreschi, G., Giugliano, M., and Grattarola, M. (1998). Analysis of the signals generated by networks of neurons coupled to planar arrays of microtransducers in simulated experiments. *Biosens. Bioelectron.* 13: 601–612.

Brunel, N. (2000). Persistent activity and the single cell f–I curve in a cortical network model. *Network* 11: 261–80.

Brunel, N. and Wang, X.J. (2003). What determines the frequency of fast network oscillations with irregular neural discharges? I. Synaptic dynamics and excitation-inhibition balance. *J. Neurophysiol.*, 90: 415–30.

Bulloch, A.G.M. and Syed, N.I. (1992). Reconstruction of neuronal networks in culture. *Trends Neurosci.*, 15: 422–27.

Canepari, M., Bove, M., Maeda, E., Cappello, M., and Kawana, A. (1997). Experimental analysis of neuronal dynamics in cultured cortical networks and transitions between different patterns of activity. *Biol. Cybern.*, 77: 153–62.

Chance, F.S., Abbott, L.F., and Reyes, A.D. (2002). Gain modulation from background synaptic input. *Neuron* 35: 773–782.

Cox, D.R. and Miller, H.D. (1965). *The Theory of Stochastic Processes*. Chapman & Hall, London.

Destexhe, A. and Paré, D. (1999). Impact of network activity on the integrative properties of neocortical pyramidal neurons *in vivo*. *J. Neurophysiol.* 81: 1531–1547.

Destexhe, A. and Paré, D. (2000). A combined computational and intracellular study of correlated synaptic bombardment in neocortical pyramidal neurons *in vivo*. *Neurocomput.* 32: 113–119.

Destexhe, A., Mainen, Z.F., and Sejnowski, T.J. (1994). Synaptic transmission and neuromodulation using a common kinetic formalism. *J. Comp. Neurosci.*, 1: 195–230.

Destexhe, A., Rudolph, M., and Paré, D. (2003). The high-conductance state of neocortical neurons *in vivo*. *Nature Rev.* 4: 739–51.

Douglas, R.J. and Martin, K.A. (1990). Neocortex. In: *The Synaptic Organization of the Brain: 3rd edition.* Oxford University Press, New York, Chap. 12, pp. 389–438.

Fleidervish, I., Friedman, A., and Gutnick, M.J. (1996). Slow inactiavation of Na^+ current and slow cumulative spike adaptation in mouse and guinea–pig neocortical neurones in slices. *J. Physiol.* 493.1: 83–97.

Fourcaud, N. and Brunel, N. (2002). Dynamics of the firing probability of noisy integrate-and-fire neurons. *Neural Comp.* 14: 2057–2110.

Fourcaud-Trocmé, N., Hansel, D., van Vreeswijk, C., and Brunel, N. (2003). How spike generation mechanisms determine the neuronal response to fluctuating inputs. *J. Neurosci.*, 23(37): 11628–11640.

Fuhrmann, G., Markram, H., and Tsodyks, M. (2002). Spike frequency adaptation and neocortical rhythms. *J. Neurophysiol.* 88: 761–770.

Fusi, S. and Mattia, M. (1999). Collective behavior of networks with linear (VLSI) integrate and fire neurons. *Neural Comp.* 11: 633–652.

Gerstein, G.L. and Mandelbrot, B. (1964). Random walk models for the spike activity of a single neuron. *Biophys. J.* 4: 41–68.

Gerstner, W. (2000). Population dynamics of spiking neurons: Fast transients, asynchronous states, and locking. *Neural Comp.* 12: 43–89.

Giugliano, M. (2000). Synthesis of generalized algorithms for the fast computation of synaptic conductances with Markov kinetic models in large network simulations. *Neural Comput.* 12(4): 771–799.

Giugliano, M., Darbon, P., Arsiero, M., Lüscher, H.-R., and Streit, J. (2004). Single-neuron discharge properties and network activity in dissociated cultures of neocortex. *J. Neurophysiol.* 92(2): 977–996.

Giugliano, M., La Camera, G., Rauch, A., Lüscher, H.-R., and Fusi, S. (2002). Non-monotonic current-to-rate response function in a novel integrate-and-fire model neuron. In: Dorronsoro, J.R., ed., *Proceedings of ICANN2002*, Springer, New York, pp. 141–146.

Grattarola, M. and Martinoia, S. (1993). Modeling the neuron-microtransducer junction: From extracellular to patch recording. *IEEE Trans. Biomed. Eng.* 40: 35–41.

Grattarola, M. and Massobrio, G. (1998). *Bioelectronics Handbook: MOSFETs, Biosensors, Neurons*. McGraw-Hill, New York.

Gross, G.W. (1979). Simultaneous single-unit recording in vitro with a photoetched laser deinsulated, gold multielectrode surface. *IEEE Trans. Biomed. Eng.* 26: 273–279.

Gross, G.W., Wen, W., and Lin, J. (1985). Transparent indium-tin oxide patterns for extracellular, multisite recordings in neuronal cultures. *J. Neurosci. Meth.* 15: 243–252.

Hamill, O.P., Marty, A., Neher, E., Sakmann, B., and Sigworth, F.J. (1981). Improved patch-clamp techniques for high-resolution current recording from cells and cell-free membrane patches. *Pfluegers Arch.* 391: 85–100.

Hodgkin, A.L. and Huxley, A.F. (1952). A quantitative description of membrane current and its application to conduction and excitation in nerve. *J. Physiol.* 117: 500–544.

Holt, G.R., Softky, W.R., Koch, C., and Douglas, R.J. (1996). Comparison of discharge variability in vitro and in vivo in cat visual cortex neurons. *J. Neurophysiol*. 75(5): 1806–1814.

Huettner, J.E. and Baughman, R.W. (1986). Primary culture of identified neurons from the visual cortex of postnatal rats. *J. Neurosci.* 6: 3044–3060.

Jimbo, Y., Tateno, T., and Robinson, H.P.C. (1999). Simultaneous induction of pathway-specific potentiation and depression in networks of cortical neurons. *Biophys. J.* 76: 670–678.

Kamioka, H., Maeda, E., Jimbo, Y., Robinson, H.P.C., and Kawana, A. (1996). Spontaneous periodic synchronized bursting during formation of mature patterns of connections in cortical cultures. *Neurosci. Lett.* 206: 109–112.

La Camera, G., Rauch, A., Senn, W., Lüscher, H.-R., and Fusi, S. (2002). Firing rate adaptation without losing sensitivity to fluctuations. In: Dorronsoro, J.R., ed., *Proceedings of ICANN2002,* Springer, New York, pp. 180–185.

La Camera, G., Senn, W., and Fusi, S. (2003). Equivalent networks of conductance- and current-driven neurons. In: *Proceedings of ICANN/ICONIP,* Instanbul, Turkey.

Maeda, E., Kuroda, Y., Robinson, H.P.C., and Kawana, A. (1998). Modification of parallel activity elicited by propagating bursts in developing networks of rat neocortical neurones. *Eur. J. Neurosci.* 10: 488–496.

Maeda, E., Robinson, H.P., and Kawana, A. (1995). The mechanisms of generation and propagation of synchronized bursting in developing networks of cortical neurons. *J. Neurosci.* 15(10): 6834–6845.

Mainen, Z.F. and Sejnowski, T. (1995). Reliability of spike timing in neocortical neurons. *Science*, 268: 1503.

Marom, S. and Shahaf, G. (2002). Development, learning and memory in large random networks of cortical neurons: lessons beyond anatomy. *Quart. Rev. Biophys.* 35: 63–87.

Mattia, M. and Del Giudice, P. (2002). Population dynamics of interacting spiking neurons. *Phys. Rev. E* 66(5): 051917.

McCormick, D.A., Connors, B.W., Lightfall, J.W., and Prince, D.A. (1985). Comparative electrophysiology of pyramidal and sparsely spiny stellate neurons of the neocortex. *J. Neurophysiol.* 59: 782–806.

Milo, R., Shen-Orr, S., Itzkovitz, S., Kashtan, N., Chklovskii, D., and Alon, U. (2002). Network motifs: Simple building blocks of complex networks. *Science*, 298(5594): 824–827.

Muramoto, K., Ichikawa, M., Kawahara, M., Kobayashi, K., and Kuroda, Y. (1993). Frequency of synchronous oscillations of neuronal activity increases during development and is correlated to the number of synapses in cultured cortical neuron networks. *Neurosci. Lett.* 163: 163–165.

Nakanishi, K. and Kukita, F. (1998). Functional synapses in synchronized bursting of neocortical neurons in culture. *Brain Res.*, 795(1–2): 137–146.

Nakanishi, K., Kukita, F., Asai, K., and Kato, T. (2001). Recurrent subthreshold electrical activities of rat neocortical neurons progress during long-term culture. *Neurosci. Lett.* 304(1–2): 85–88.

Nakanishi, K., Nakanishi, M., and Kukita, F. (1999). Dual intracellular recording of neocortical neurons in a neuron-glia co-culture system. *Brain Res. Prot.* 4: 105–114.

Poliakov, A.V., Powers, R.K., and Binder, M.D. (1997). Functional identification of the input-output transforms of motoneurones in the rat and cat. *J. Physiol.* 504.2: 401–424.

Potter, S.M. and DeMarse, T.B. (2001). A new approach to neuronal cell culture for long-term studies. *J. Neurosci. Meth.* 59: 782–806.

Powers, R.K., Sawczuk, A., Musick, J.R., and Binder, M.D. (1999). Multiple mechanisms of spike-frequency adaptation in motoneurones. *J.Physiol. (Paris)* 93: 101–114.

Press, W., Teukolsky, S.A., Vetterling, W.T., and Flannery, B.P. (1992). *Numerical Recipes in C: The Art of Scientific Computing*. Cambridge University Press, New York.

Protopapas, A.D. and Bower, J.M. (2001). Spike coding in pyramidal cells of the piriform cortex of rat. *J. Neurophysiol.* 86: 1504–1510.

Rauch, A., La Camera, G., Lüscher, H.-R., Senn, W., and Fusi, S. (2003). Neocortical pyramidal cells respond as integrate-and-fire neurons to *in vivo*-like input currents. *J. Neurophysiol.* 90: 1598–1612.

Reutimann, J., Giugliano, M., and Fusi, S. (2003). Event-driven simulation of spiking neurons with stochastic dynamics. *Neural Comp.* 15: 811–830.

Ricciardi, L.M. (1977). *Diffusion Processes and Related Topics in Biology*. Springer, Berlin.

Risken, H. (1984). *The Fokker–Planck Equation: Methods of Solution and Applications*. Springer, Berlin.

Robinson, H.P.C., Kawahara, M., Jimbo, Y., Torimitsu, K., Kuroda, Y., and Kawana, A. (1993). Periodic synchronized bursting and intracellular calcium transients elicited by low magnesium in cultured cortical neurons. *J. Neurophysiol.* 70: 1606–1616.

Salinas, E. (2003). Background synaptic activity as a switch between dynamical states in a network. *Neural Comp.* 15: 1439–1475.

Sanchez-Vives, M.V. and McCormick, D.A. (2000). Cellular and network mechanisms of rhythmic recurrent activity in neocortex. *Nat. Neurosci.* 3: 1027–1034.

Sanchez-Vives, M.V., Nowak, L.G., and McCormick, D.A. (2000). Cellular mechanisms of long-lasting adaptation in visual cortical neurons *in vitro*. *J. Neurosci.* 20: 4286–4299.

Sawczuk, A., Powers, R.K., and Binder, M.D. (1997). Contribution of outward currents to spike frequency adaptation in hypoglossal motoneurons of the rat. *J. Physiol.* 78: 2246–2253.

Schwindt, P.C., Spain, W.J., and Crill, W.E. (1989). Long-lasting reduction of excitability by a sodium-dependent potassium current in cat neocortical neurons. *J. Neurophysiol.* 61: 233–244.

Shadlen, M.N. and Newsome, W.T. (1998). The variable discharge of cortical neurons: implications for connectivity, computation, and information coding. *J. Neurosci.* 18(10): 3870–3896.

Silberberg, G., Bethge, M., Markram, H., Pawelzik, K., and Tsodyks, M. (2004). Dynamics of population rate codes in ensembles of neocortical neurons. *J. Neurophysiol.* 91(2): 704–709.

Smith, G.D., Cox, C.L., Sherman, S. M., and Rinzel, J. (2000). Fourier analysis of sinusoidally driven thalamocortical relay neurons and a minimal integrate-and-fire-or-burst model. *J. Neurophysiol*. 83(1): 588–610.

Stengler, D.A. and McKenna, T.M. (1994). *Enabling Technologies for Cultured Neural Networks*. Academic Press, London.

Steriade, M. (2001). Similar and contrasting results from studies in the intact and sliced brain. In: *The Intact and Sliced Brain*, Bradford Books, MIT Press, Cambridge, MA, Chap. 3, pp. 103–190.

Streit, J., Tscherter, A., Heuschkel, M.O., and Renaud, P. (2001). The generation of rhythmic activity in dissociated cultures of rat spinal cord. *Eur. J. Neurosci.* 14: 191–202.

Tscherter, A., Heuschkel, M.O., Renaud, P., and Streit, J. (2001). Spatiotemporal characterization of rhythmic activity in spinal cord slice cultures. *Eur. J. Neurosci.* 14: 179–190.

Tsodyks, M., Uziel, A., and Markram, H. (2000). Synchrony generation in recurrent networks with frequency-dependent synapses. *J. Neurosci.* 20: RC50: 1–5.

Tuckwell, H.C. (1988). *Introduction to Theoretical Neurobiology*. Cambridge University Press, New York.

Turrigiano, G.G. and Nelson, S.B. (2004). Homeostatic plasticity in the developing nervous system. *Nature Rev. Neurosci.* 5(2): 97–107.

Van den Pol, A.N., Obrietan, K., and Belousov, A. (1996). Glutammate hyperexcitability and seizure-like activity throughout the brain and spinal cord upon relief from chronic glutammate receptor blockade in culture. *Neuroscience* 74: 653–674.

Van Huizen, F., Romijn, H.J., and Corner, M.A. (1987). Indications for a critical period for synapse elimination in developing rat cerebral cortex cultures. *Brain Res.*, 428: 1–6.

Van Vreeswijk, C., and Hansel, D. (2001). Patterns of synchrony in neural networks with spike adaptation. *Neural Comp.* 13: 959–992.

Wang, X.J. (2001). Synaptic reverberation underlying mnemonic persistent activity. *Trends Neurosci.* 24(8): 455–463.

Wiedemann, U.A. and Lüthi, A. (2003). Timing of network synchronization by refractory mechanisms. *J. Neurophysiol.* 90: 3902–3911.